AIP Journal of Applied Physics

# Dynamics of laser-induced phase switching in GeTe films

W. Gawelda, J. Siegel, C. N. Afonso, V. Plausinaitiene, A. Abrutis et al.

Citation: J. Appl. Phys. 109, 123102 (2011); doi: 10.1063/1.3596562
View online: http://dx.doi.org/10.1063/1.3596562
View Table of Contents: http://jap.aip.org/resource/1/JAPIAU/v109/i12
Published by the American Institute of Physics.

## Related Articles

High Seebeck effects from conducting polymer: Poly(3,4-ethylenedioxythiophene):poly(styrenesulfonate) based thin-film device with hybrid metal/polymer/metal architecture
APL: Org. Electron. Photonics 5, 238 (2012)

High Seebeck effects from conducting polymer: Poly(3,4-ethylenedioxythiophene):poly(styrenesulfonate) based thin-film device with hybrid metal/polymer/metal architecture
Appl. Phys. Lett. 101, 173304 (2012)

Response to "Comment on 'Silver/silicon dioxide/silver sandwich films in the blue-to-red spectral regime with negative-real refractive index'" [Appl. Phys. Lett. 101, 156101 (2012)]
Appl. Phys. Lett. 101, 156102 (2012)

On the determination of the glass forming ability of AlxZr1−x alloys using molecular dynamics, Monte Carlo simulations, and classical thermodynamics
J. Appl. Phys. 112, 073508 (2012)

Enhanced photoanode properties of epitaxial Ti doped α-Fe2O3 (0001) thin films
Appl. Phys. Lett. 101, 133908 (2012)

## Additional information on J. Appl. Phys.

Journal Homepage: http://jap.aip.org/
Journal Information: http://jap.aip.org/about/about_the_journal
Top downloads: http://jap.aip.org/features/most_downloaded
Information for Authors: http://jap.aip.org/authors

ADVERTISEMENT

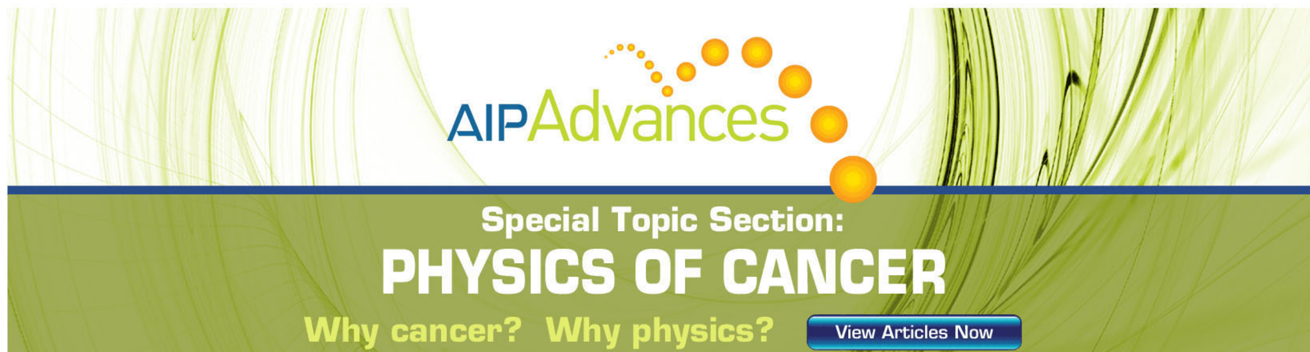


Downloaded 29 Oct 2012 to 161.111.22.141. Redistribution subject to AIP license or copyright; see http://jap.aip.org/about/rights_and_permissions

# Dynamics of laser-induced phase switching in GeTe films

W. Gawelda,[1,a),b)] J. Siegel,[1,a)] C. N. Afonso,[1] V. Plausinaitiene,[2] A. Abrutis,[2] and C. Wiemer[3]
[1]*Laser Processing Group, Instituto de Óptica, CSIC, Serrano 121, E-28006 Madrid, Spain*
[2]*Department of General and Inorganic Chemistry, Vilnius University, Naugarduko 24, LT-03225 Vilnius, Lithuania*
[3]*Laboratorio MDM, IMM-CNR, via C. Olivetti 2, 20864 Agrate Brianza, (MB) Italy*

(Received 9 March 2011; accepted 29 April 2011; published online 17 June 2011)

Phase switching in GeTe thin films (grown using a modified metal organic chemical vapor deposition system) upon pulsed femtosecond and nanosecond laser irradiation has been studied. Two *in situ* methods, i.e., optical microscopy and real-time reflectivity measurements, have been used in order to compare the optical response before and after phase change and to follow the phase change dynamics with a time resolution close to 400 ps. The results show that cycling is possible under irradiation with both fs and ns pulses using single pulses for amorphization and multiple pulses for crystallization. The use of ns pulses favors the crystalline-to-amorphous phase transformation, with a characteristic transformation time of ∼15 ns. The presence of the liquid phase was identified and temporally resolved, featuring a well-defined transient reflectivity state, in between those of the crystalline and amorphous phases. We have also studied the role of material configuration in the phase change dynamics and the mechanisms involved in the re-crystallization process. © *2011 American Institute of Physics*. [doi:10.1063/1.3596562]

## I. INTRODUCTION

Phase switching in chalcogenide alloys, containing Ge, Sb, and Te, has been extensively studied in relation to its application in optical data storage technology.[1] Chalcogenides have also been proposed as suitable materials for the next generation of electrically addressed phase change memory (PCM) devices.[2] The basic mechanism of PCM relies on reversible switching between amorphous and crystalline phases, characterized by significantly different optical[3] and electrical[4] properties. Phase transformations can be triggered by means of short optical laser or electrical current pulses and are characterized by large differences in optical reflectivity or electrical resistivity, respectively. In both cases, the phase transition from an amorphous to a crystalline state (a → c) and vice-versa, i.e., a crystalline to an amorphous state (c → a), requires controlled heating and cooling conditions, which determine the transformation path. Because the c → a process requires rapid melting and quenching, short (picosecond, ps) or even ultrashort (femtosecond, fs) optical pulses are inherently preferable as compared to nanosecond (ns) laser pulses because they yield much higher cooling rates. In contrast, the inverse transformation (a → c) is favored by longer pulses due to the minimum time required for stable crystalline nuclei to form and grow.[5]

Over past decades, binary alloys such as GeTe and $Sb_2Te_3$ and ternary alloys, located along the GeTe–$Sb_2Te_3$ pseudobinary line, were intensively studied both theoretically[6] and experimentally in relation to their applications in optical phase-change data storage. These studies explored a vast number of parameters including pulse duration,[7] wavelength,[8] pulse energies,[9] the role of oxygen impurities,[10] vacancies,[11] and local structure.[12] Time-resolved optical studies using ps and fs laser pulses have already revealed important details of the phase transition, such as the existence of three distinct stages, namely, rapid melting, solidification, and slow relaxation.[13] In addition, it was found that optical techniques are well suited for optimizing heat-flow conditions in $Ge_{0.07}Sb_{0.93}$ (Ref. 14) and $Ge_2Sb_2Te_5$ (Ref. 15) films by tailoring the thermal conductivity of the substrate to either facilitate or prevent amorphization. Although the pseudobinary GeTe–SbTe alloy (and especially the $Ge_2Sb_2Te_5$ composition) is the best known candidate for PCMs,[16] both of its binary constituents, i.e., GeTe and $Sb_2Te_3$, have also demonstrated potential for phase change recording.[17,18] GeTe in particular has received increasing industrial interest as an active material in electrical PCMs, especially in nonvolatile memory devices.[19] Recently, Raoux *et al.*[20] reported an extensive study on crystallization times in GeTe films produced via rf sputtering as a function of alloy composition. They confirmed earlier reports, by Chen *et al.*,[5] that crystallization times for compositions other than the stoichiometric one increase by orders of magnitude, and they underlined the role played by the melt-quenched amorphous phase in the fast re-crystallization process.

The metal organic chemical vapor deposition system (MOCVD) is a promising method to address the targeted downscaling of device structures because it is conceptually capable of providing better control of the film deposition over nonplanar structures (conformality) and better composition control. This aspect is paramount in modern PCMs because their geometry is based on micro-trenches that are covered by a thin film of a chalcogenide material and which act as a unit active block of a memory device. Therefore, high-quality control over the composition, conformality, and increased

[a)]Authors to whom correspondence should be addressed. Electronic addresses: wojciech.gawelda@xfel.eu and j.siegel@io.cfmac.csic.es.
[b)]Present address: European XFEL GmbH, Albert-Einstein-Ring 19, 22761 Hamburg, Germany.

 © 2011 American Institute of Physics

Downloaded 29 Oct 2012 to 161.111.22.141. Redistribution subject to AIP license or copyright; see http://jap.aip.org/about/rights_and_permissions

manufacturing throughput are desired as compared to direct physical vapor deposition techniques, such as rf sputtering techniques.

The aim of this work is to study the laser-induced phase switching behavior in GeTe films produced using a modified version of MOCVD, i.e., hot wire pulsed liquid injection MOCVD (HW-LI-MOCVD),[21] in order to evaluate their phase switching performance and dynamics. Moreover, we verify the phase switching feasibility not only with conventional ns but also with fs laser pulses. The study uses *in situ* optical microscopy as a rapid assessment tool for the optical characterization of phase switching conditions by comparing the optical response before and after phase change, as obtained from microscopy images with real-time reflectivity (RTR) measurements at the irradiated area center used to follow the phase change dynamics with a time resolution close to 400 ps. This allows one to characterize, with spatial resolution, the mechanisms that govern the amorphization and re-crystallization processes.

## II. EXPERIMENTAL DETAILS

The experimental setup uses a commercial femtosecond Ti:sapphire regenerative amplifier system to induce phase changes. For irradiation with fs pulses, the system was operated in a standard configuration providing $\tau = 120$ fs pulses. For irradiation with ns pulses, the amplifier was operated in a Q-switched mode without seed pulses, thus providing 8 ns pulses at the same wavelength ($\lambda = 800$ nm). The s-polarized beam was then focused onto the sample at an angle of incidence of 53° to an elliptical spot size of $100 \times 59$ $\mu m^2$ ($1/e^2$ intensity diameters). Because the spatial profile of the pump beam is Gaussian, it translates into a Gaussian intensity distribution in the focus at the sample surface and thus allows one to analyze the reflectivity changes corresponding to different local fluences along the image profile (see the inset of Fig. 1(a)). The irradiation fluence was adjusted by changing the pump pulse energy using a combination of a $\lambda/2$ waveplate and a polarizer. The laser fluence values used in the experiments refer to peak fluences in front of the sample.

We used a single laser pulse, selected from a 100 Hz pulse train by means of an electromechanical shutter, to irradiate unexposed regions of the sample. The induced phase change was observed *in situ* with an optical microscope as shown in Fig. 1(a). The microscope is composed of a long working distance objective lens [numerical aperture (NA) = 0.42] and a tube lens (in a configuration along the normal to the sample surface), which allows one to record magnified images (× 20) on a 12-bit CCD camera using a white-light emitting diode as a source. The temporal evolution of the reflectivity changes was monitored with a frequency-doubled, continuous-wave, single-frequency Nd:YAl garnet laser emitting at 532 nm, the output of which was focused to a spot size of $\sim 5 \times 5$ $\mu m^2$ at the center of the irradiated region [Fig. 1(b)]. The specular reflection of the probe light was recorded simultaneously by two detectors: a fast photodiode (PD) and a streak camera (SC), yielding transient reflectivity changes as a function of time, as shown in the insets of Fig. 1(b). Here, some representative reflectivity traces are shown as recorded in GeTe films, showing how the temporal resolution improves when switching from a PD (tens of ns) to a SC detector ($\geq$400 ps). Further details of the detection system can be found in Ref. 22.

GeTe thin films were grown via the HW-LI-MOCVD technique using diluted solutions of $Ge[N(CH_3)_2]_4$ and $Te(i\text{-}C_3H_7)_2$ precursors in toluene. Unless otherwise specified, the results reported in this work were obtained in $Ge_{0.46}Te_{0.54}$ films (15 to 20 nm thick) deposited at 300 °C on Si wafers covered by a 10 nm thick buffer layer of $SiO_2$. In order to evidence the importance of the material configuration (i.e., film and buffer layer thicknesses) to the phase change behavior, a thicker (50 nm)

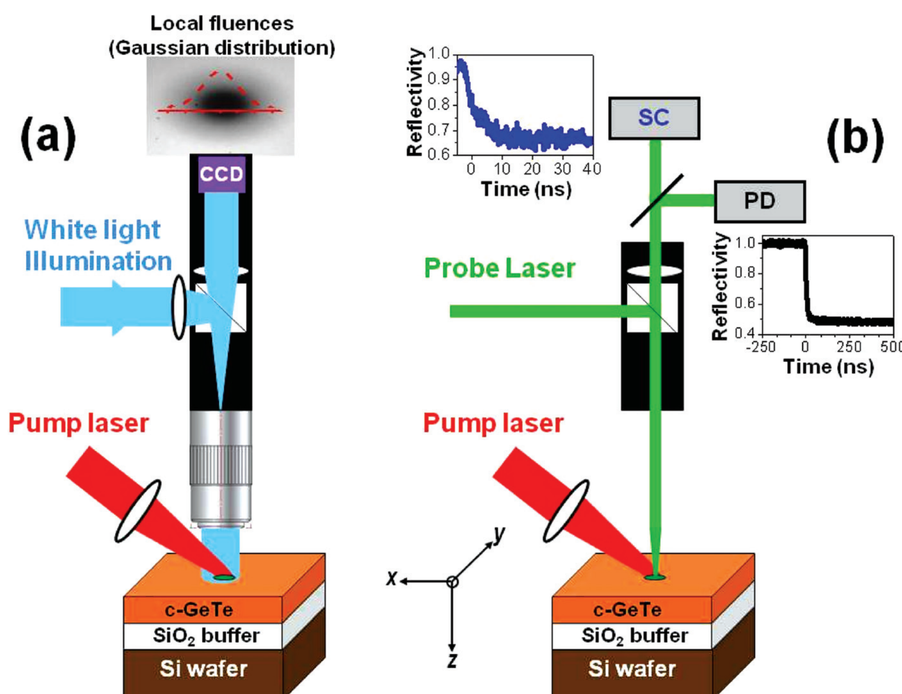


FIG. 1. (Color online) The experimental setup used for combined (a) *in situ* optical microscopy and (b) time-resolved reflectivity measurements. The pump beam (800 nm with a pulse duration of either 120 fs or 8 ns) is focused (NA = 0.42 objective) on the sample surface. (a) An incoherent white-light source or (b) a CW laser at 532 nm is used for probing the spatial and temporal behavior of the photoinduced reflectivity changes. In (b), the probe beam is detected with either a fast photodiode (PD) or a streak camera (SC), which allows one to record laser-induced relative reflectivity changes with different temporal resolution (from ns down to ps resolution).

Downloaded 29 Oct 2012 to 161.111.22.141. Redistribution subject to AIP license or copyright; see http://jap.aip.org/about/rights_and_permissions

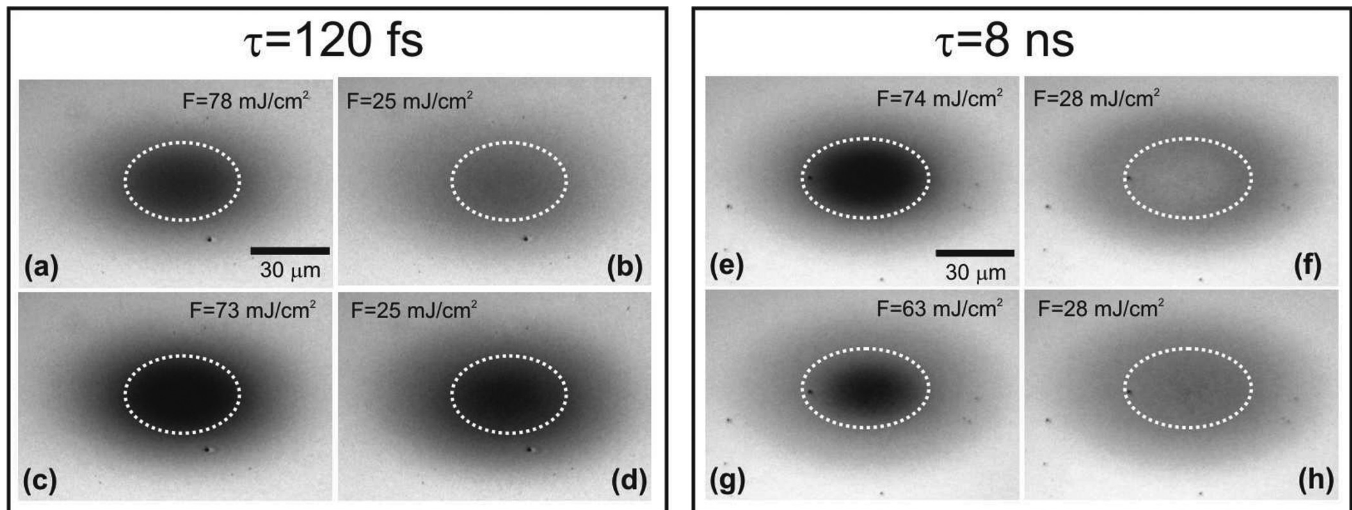


FIG. 2. A series of images of (a)-(d) femtosecond and (e)-(h) nanosecond laser-irradiated surfaces of $Ge_{0.46}Te_{0.54}$ thin films. In (a) and (e), the photoinduced reflectivity change to a low-reflectivity state upon exposure to an intense SP irradiation is shown. The partial recovery of the initial high-reflectivity state is depicted in (b) and (f) upon MP irradiation using multiple pulses. The subsequent cycling between both states is shown in images (c) and (d) upon fs laser irradiation, and in (g) and (h) using ns pulses. The field of view in all images is $120 \times 80\ \mu m^2$.

film on a thicker (30 nm) $SiO_2$ buffer layer was also produced. The as-deposited films were polycrystalline. Crystallization occurs in the rhombohedral phase of GeTe.[21] Energy dispersive spectroscopy analysis confirmed an almost stoichiometric composition (Ge 46%, Te 55%). Atomic force microscopy study revealed a rather smooth surface with an average roughness value of $R_a \approx 2$ nm. A more detailed description of the film growth process is provided elsewhere.[23]

## III. RESULTS AND DISCUSSION

### A. *In situ* microscopy

White light illumination images of the sample upon single fs and ns laser pulse irradiation recorded in reflection with the *in situ* microscope [Fig. 1(a)] are shown in Fig. 2 and correspond to consecutive irradiations of the same sample spot. These images are used for the initial optical characterization of the laser-irradiated films and help in assessing rapidly the phase-change behavior of the selected thin-films, particularly when studying the spatial features.

For both pulse durations, the first images shown in Figs. 2(a) and 2(e) correspond to a single pulse (SP) irradiation with high fluence, which induces a dark region related to amorphization, as confirmed using Raman spectroscopy.[24] The second images in Figs. 2(b) and 2(f) correspond to multiple pulse (MP) irradiation (>500 pulses) of the transformed areas in Figs. 2(a) and 2(e) using low fluence, which leads to a brighter region as compared to the first images. This behavior is consistent with re-crystallization, although the region is slightly darker than that of the as-grown phase. The third images in Fig. 2(c) and 2(g) correspond to the irradiated areas in Figs. 2(b) and 2(f) with a SP of fluence similar to that in Figs. 2(a) and 2(e), which results in a similar dark region, i.e., amorphization. Finally, images in Figs. 2(d) and 2(h) correspond to MP irradiation of the area in Figs. 2(c) and Fig. 2(g). While the latter has a contrast similar to that in Fig. 2(f), i.e., slightly darker than that of the as-grown area, the former shows a much darker contrast. For both fs- and ns-irradiated films, we have observed reversible optical switching with considerable optical contrast (OC). OC is defined as a difference in the normalized reflectivities of the non-irradiated crystalline film (as-grown) and the center of the irradiated region, namely, $OC = R_{norm}(cryst) - R_{norm}(irr\text{-}center) = 1 - R_{norm}(irr\text{-}center)$. This is better appreciated in Fig. 3, which shows the normalized spatial reflectivity profiles across the irradiated spot center extracted from the images in Fig. 2 for both fs [Fig. 3(a)] and ns [Fig. 3(b)] laser pulses.

A gradual decrease of the reflectivity difference between the laser-induced amorphous and crystalline phases upon fs irradiation is observed. In contrast, the OC difference is preserved upon ns irradiation for similar fluences. This result is consistent with the beneficial effect of long pulses on the

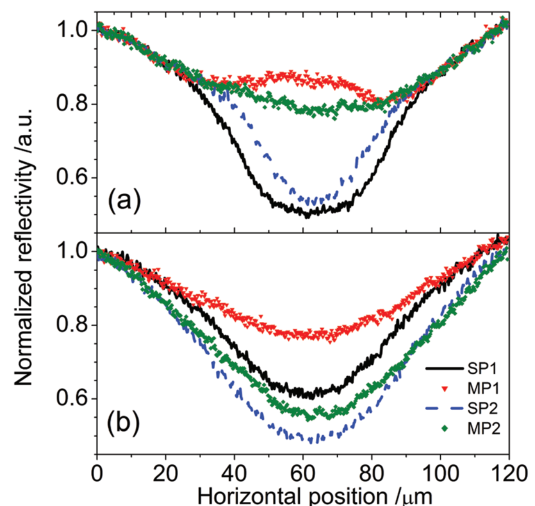


FIG. 3. (Color online) Spatial reflectivity profiles of GeTe films irradiated with (a) ns and (b) fs laser pulses. The reflectivity difference between the laser-induced amorphous phase (SP1) and the re-crystallized (MP1) state defines the optical contrast.

Downloaded 29 Oct 2012 to 161.111.22.141. Redistribution subject to AIP license or copyright; see http://jap.aip.org/about/rights_and_permissions

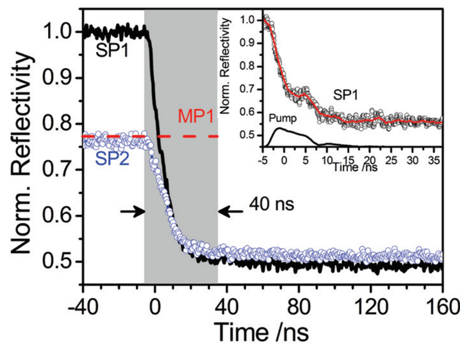


FIG. 4. (Color online) RTR changes of the ns laser-irradiated GeTe thin films recorded using the setup from Fig. 1(b). The observed reflectivity changes are assigned to a SP c → a phase transformation (SP1 and SP2) and were recorded using a PD detector. The re-crystallized reflectivity level (MP1) is indicated with a dashed line. The inset zooms into the reflectivity changes upon SP amorphization using a picosecond SC detector (SP1) in a 40 ns time window, indicated by the gray area. The temporal profile of the ns pump pulse is shown for comparison.

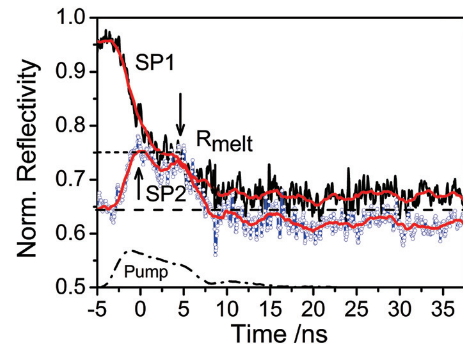


FIG. 5. (Color online) Transient reflectivity changes of the ns laser-irradiated GeTe thin films during c → a transformation recorded using a SC detector. The SP1 trace shows the amorphization dynamics, and the dashed horizontal line marks the final amorphous low-reflectivity state. The effect of melting the amorphous GeTe is shown in the SP2 trace. The temporal profile of the pump pulse is shown toward the bottom of the graph (dashed curve).

crystallization, most likely related to the lower heating/cooling rates involved, and evidences that phase switching is considerably better for ns than for fs laser pulse irradiation.

### B. Real-time reflectivity measurements

In view of the above-discussed results, RTR measurements to study the phase transformation dynamics/kinetics were obtained only upon irradiation with 8 ns pulses. Figure 4 shows the normalized reflectivity transient measured with ns-resolution using a PD detector upon SP1 irradiation at 71 mJ/cm$^2$, for which a very fast substantial decrease of 50% of the initial reflectivity is observed, similar to the results shown in Fig. 2(e). The observed transformation time is close to the temporal resolution limit of the PD detector. The reflectivity decrease is attributed to melting followed by amorphization of the as-grown GeTe. Subsequent MP irradiation at 30 mJ/cm$^2$ (the final level is indicated with a solid line MP1) partially recovers the high-reflectivity state because the re-crystallized phase is characterized by lower reflectivity (0.77). Subsequent SP irradiation with 62 mJ/cm$^2$ (SP2) switches the material back to the low-reflectivity state. In both cases, the photoinduced amorphous state has a constant reflectivity (0.5). The actual transformation times of the amorphization process could be better resolved by using the SC detector. The gray area in Fig. 4 shows the temporal window of 40 ns, where ps-resolved RTR measurements with a SC detector were carried out (inset Fig. 4). The pump pulse is shown below the reflectivity transients for comparison. The remarkable feature observed in the SP1 trace in the inset of Fig. 4 is an intermediate plateau at ~5 ns after the laser pulse. It has been shown in other chalcogenide films that this transient intermediate level corresponds to the presence of the molten phase, because laser-induced amorphization requires melting as a preceding step before the crystalline-amorphous phase transition occurs.[25]

In order to resolve more clearly the plateau related to the molten state, we have used two consecutive single pulses at high fluence—the first one to melt and amorphize the film as before, the second one to melt the amorphous phase and re-amorphize the film. The recorded reflectivity transients are shown in Fig. 5. The first SP1 irradiation (75 mJ/cm$^2$) triggers a crystalline–liquid–amorphous (c → l → a) transition featuring, as in the inset of Fig. 4, a plateau of constant reflectivity corresponding to the liquid phase. The subsequent SP2 irradiation at 81 mJ/cm$^2$ melts the amorphous layer and re-solidifies it into the amorphous phase (a → l → a).

The intermediate reflectivity $R_{melt}$ of the liquid phase (marked by a dotted horizontal line in Fig. 5) between the as-grown crystalline state and the photoinduced amorphous state is clearly appreciable upon irradiation with SP2. Its temporal evolution and duration agree consistently with those of the amorphization process during SP1. After melting, the liquid phase re-solidifies to the initial solid state, in this case to the amorphous state. The c → l transformation time obtained upon SP1 in Fig. 5 is ≈5 ns, which was extracted as the time interval between the initial reflectivity decrease and the appearance of the melt. This implies that the rising edge of the 8 ns FWHM pulse triggers the formation of an optically thick molten layer, and complete melting is achieved in ca. 3 ns (the first maximum in the SP2 trace in Fig. 5). The relatively long duration of the reflectivity plateau (ca. 5 ns) indicates that the melt persists for the entire duration of the pump pulse, and the re-solidification time (the reflectivity decrease in the SP2 trace in Fig. 5) amounts to approximately 3 ns. Furthermore, Fig. 5 shows that the reflectivity of the liquid phase $R_{melt}$ is 0.75 $R_c$, where $R_c$ describes the crystalline phase.

### C. Quantification of the optical contrast

In order to extract the OC as a function of the pump fluence, we have performed a series of fluence-dependent measurements of the c → a phase transformation upon single-pulse ns irradiation under identical experimental conditions. During these measurements, we have gradually increased the laser fluence in the 28-90 mJ/cm$^2$ range, exposing a fresh region to each laser pulse. For each fluence, we recorded a corresponding image using the *in situ* white-light microscopy setup shown in Fig. 1(a). From these images, reflectivity values in the spot center were extracted and

Downloaded 29 Oct 2012 to 161.111.22.141. Redistribution subject to AIP license or copyright; see http://jap.aip.org/about/rights_and_permissions

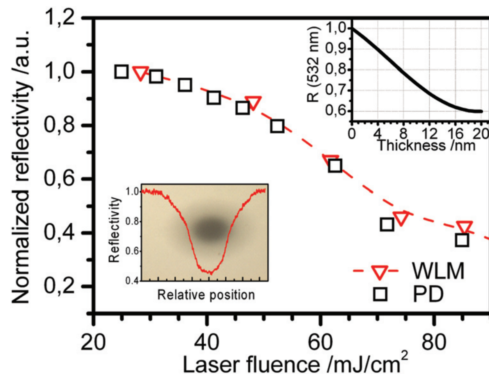


FIG. 6. (Color online) Optical reflectivity changes as a function of the incident laser pulse fluence, measured using white light (triangles) and at 532 nm (squares). The inset white-light microscope (WLM) image shows the amorphized GeTe surface change upon 74 mJ/cm$^2$ ns single-pulse irradiation. The horizontal cross section of the image yields a normalized reflectivity profile. In the inset, calculated reflectivity changes (at 532 nm) upon amorphization of GeTe thin film are shown as a function of the GeTe thickness.

normalized to the value of the unexposed sample (open triangles), thus yielding the corresponding value of the OC. The results are summarized in Fig. 6, where the dashed line is an interpolation that serves only to highlight the decreasing trend of the measured reflectivity.

At fluences $\leq$30 mJ/cm$^2$, no change in the OC can be appreciated. Above this fluence, a continuous increase of the OC as laser fluence increases is observed up to ca. 85 mJ/cm$^2$. For fluences > 50 mJ/cm$^2$ (image not shown here), *in situ* microscope (WLM) images show a partially amorphized surface upon SP irradiation. Increasing the fluence up to 74 mJ/cm$^2$ develops a clearly visible (dark ellipse) amorphous layer on the film surface, as indicated in the lower inset in Fig. 6. For higher fluences (>85 mJ/cm$^2$), ablation occurred, as was verified using the same setup. OC extracted from *in situ* microscopy is compared to reflectivity changes at the spot center measured with a PD detector (open squares), and they show a good agreement. Such agreement simplifies the analysis because in both systems different wavelengths were used and the optical properties of the sample could be wavelength dependent. Since the measured reflectivity change during the c $\rightarrow$ a phase transformation reflects the corresponding change in the complex refractive index ($n+ik$), we have calculated the expected reflectivity change for a thin film of crystalline GeTe on a $SiO_2$(10 nm)/c-Si substrate upon amorphization of the as-grown crystalline alloy. Calculations of the induced reflectivity changes were performed, taking into account the wavelength of the probe laser (532 nm) and the optical constants of the substrate and the involved phases of the film material (amorphous and crystalline), using the values of the real and imaginary parts of the complex refractive index reported in Ref. 26. This has been done by means of a direct calculation, using Fresnel formulae, of the reflectivity evolution for a monochromatic electromagnetic wave interacting with a multilayered system formed by a crystalline GeTe film on a Si substrate when the film converts, layer by layer, starting from the surface, into the amorphous phase. The code calculates the reflectivity of the whole system at the monitoring wavelength as a function of the transformation depth. The results are shown in the upper inset of Fig. 6, where it is observed that the maximum change of the OC is equal to $\Delta R=0.6$ at 532 nm for a transformed film thickness of 20 nm. This OC is slightly lower than the experimentally observed values of $\Delta R=0.5$, at an irradiation fluence of 71 mJ/cm$^2$, and $\Delta R=0.45$ (73 mJ/cm$^2$) shown in Figs. 4 and 6, respectively. This discrepancy might result from the presence of an amorphous component, as already detected in as-grown samples via Raman spectroscopy.[24]

### D. Study of the re-crystallization mechanism

Figure 2 shows that re-crystallization of the melt-quenched phase is possible, but only upon MP laser irradiation. According to the recent study in Ref. 20, it can be expected that crystallization upon single laser pulse irradiation can be achieved only with pulses >30 ns. In order to achieve crystallization with shorter pulses, additional optimization of the heat-flow conditions is required.[15] We have carried out a study of progressive crystallization upon irradiation with 8 ns pulses in samples with the same GeTe composition but with a larger film thickness (50 nm) and a thicker $SiO_2$ buffer layer (30 nm). In Figs. 7(a)–7(d), a sequence of consecutive images showing the gradual re-crystallization process is presented. Similar to Fig. 2, the film is first amorphized upon ns SP1, which is evidenced by the appearance of an area with low reflectivity at the center of Fig. 7(a). Upon subsequent

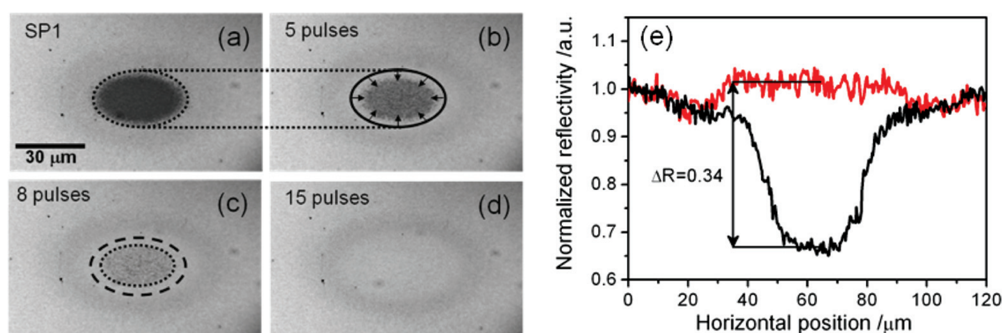


FIG. 7. (Color online) A series of images upon MP irradiation with ns laser pulses of a thicker sample. Upon intense SP irradiation, (a) an amorphous spot is induced at the center part of the laser focus. Subsequent low-fluence MP irradiation with a total of (b) 5, (c) 8, and (d) 15 pulses shows the re-crystallization process of the melt-quenched amorphous spot. Spatial reflectivity profiles corresponding to the images shown in (a) and (d) are depicted in (e), and the vertical arrow indicates the observed OC.

Downloaded 29 Oct 2012 to 161.111.22.141. Redistribution subject to AIP license or copyright; see http://jap.aip.org/about/rights_and_permissions

irradiation with 5 low-fluence pulses [Fig. 7(b)], at F = 28 mJ/$cm^2$, the re-crystallization of the melt-quenched amorphous phase initiates at the boundary of the crystalline–amorphous interface towards the center of the transformed area, and it is thus an interface controlled process. Additional 3 pulses shows instead that bulk nucleation of the crystalline phase is occurring at the central region, with no significant progress of the above-mentioned interface controlled process [Fig. 7(c)]. After the accumulation of 15 laser pulses, the entire initially amorphous spot is re-crystallized [Fig. 7(d)]. The fact that the inner region in Fig. 7(b) is brighter than that in Fig. 7(a) suggests that although an interface controlled process appear dominant in the first pulses, nucleation controlled processes have also occurred at the central area.[27] The re-crystallized surface can be re-amorphized upon another SP irradiation (not shown here) in subsequent phase switching cycles. Spatial reflectivity profiles, taken along the horizontal axis of the irradiated areas in Figs. 7(a) and 7(d), are shown for comparison in Fig. 7(e). These profiles can be compared with the spatial profiles in Fig. 3 showing some appreciable differences in radial reflectivity changes, i.e., a smooth radial transition in 20-nm films (Fig. 3) and a sharp reflectivity decrease in thicker films [Fig. 7(e)]. We can only qualitatively attribute these changes to the film thickness, as thinner films are subject to larger cooling rates due to faster heat dissipation to the substrate. The observed OC is smaller than in the case of thinner samples, most likely due to different thermodynamical conditions in this film configuration as well. As already shown by our simulations (upper inset in Fig. 6), the maximum OC for 20-nm GeTe films requires a fully transformed film thickness (the entire GeTe layer is melted), and thus it is assumed that the amorphous layer is in contact with the substrate. This means that heat-flow conditions will be different than in the case of a sample with a 50-nm GeTe layer. Moreover, the initial reflectivity decreases upon SP c → a transition, and the re-crystallized phase has a slightly higher reflectivity value than the as-grown phase. This clearly indicates that the as-grown material was partially amorphous and that MP irradiation improves the nucleation of the crystalline phase within the laser-irradiated area. Although the results shown in Fig. 7 are qualitative, they show how strongly different film geometries can influence heat-flow conditions and thus the observed re-crystallization mechanism involved in the phase transformation.

## IV. CONCLUSIONS

The study of laser-induced phase switching in GeTe thin films obtained by using a novel growth method allowed us to extract differences in the amorphization process upon fs and ns laser irradiation and valuable information about the re-crystallization mechanisms, using two complementary techniques in both steady-state and time-resolved regimes. While reversible c → a and a → c phase transitions were observed upon both fs and ns irradiation, the former pulses lead to a faster degradation of the optical contrast achieved upon phase switching due to the higher cooling rates involved.

*In situ* optical microscopy delivered space-resolved (and thus fluence-resolved) reflectivity images that allow us to quantify the OC between amorphous and crystalline phases involved in phase switching. The images also allowed us to extract the laser fluence threshold for amorphization and delivered valuable information about the re-crystallization mechanisms involved. The comparison of microscopy results with RTR measurements shows very good agreement, confirming that *in situ* optical microscopy can be regarded as a versatile tool for the rapid characterization of the optical properties involved in phase switching. Also, the dynamic studies using RTR measurements focused to the amorphization dynamics under ns pulse irradiation revealed a characteristic full transformation time of ~15 ns for a broad range of irradiation fluences. The dynamics of melting and solidification could be resolved, and take place during the c → a phase transition. The complete melt formation time was estimated to be ~3 ns, and the corresponding reflectivity change involved was determined to be $R_{melt} \approx 0.25$ with respect to the polycrystalline phase, i.e., lying between the values for polycrystalline and amorphous GeTe.

Optical microscopy was used also to study the re-crystallization process. The comparison of the OC evolution of the irradiated areas upon multiple pulse irradiations allowed us to obtain qualitative results on the involved mechanism. The re-crystallization is triggered at the interface of the amorphous and as-grown crystalline area and thus is an interface-controlled process. As the number of pulses is increased, a nucleation controlled process becomes more dominant until complete re-crystallization. Moreover, a comparison of the maximum achieved OC showed a clear dependence of the crystallization process on both film and buffer layer thickness.

## ACKNOWLEDGMENTS

This work has been partially supported by the EU project CHEMAPH (IST-027561) and by the Spanish Ministry of Education and Science (Project TEC 2008-01183). W.G. acknowledges the CSIC-I3P Programme contract co-funded by the European Social Fund.

[1] M. Wuttig and N. Yamada, Nature Mater. **6**, 824 (2007).
[2] M. H. R. Lankhorst, B. W. S. M. M. Ketelaars, and R. A. M. Wolters, Nature Mater. **4**, 347 (2005).
[3] J. Feinleib, J. De Neufville, S. C. Moss, and S. R. Ovshinsky, Appl. Phys. Lett. **18**, 254 (1971).
[4] S. R. Ovshinsky, Phys. Rev. Lett. **21**, 1450 (1968).
[5] M. Chen, K. A. Rubin, and R. W. Barton, Appl. Phys. Lett. **49**, 502 (1986).
[6] S. Yamanaka, S. Ogawa, I. Morimoto, and Y. Ueshima, Jpn. J. Appl. Phys. **37**, 3327 (1998).
[7] S. M. Wiggins, J. Solis, and C. N. Afonso, Appl. Phys. Lett. **84**, 4445 (2004).
[8] S. M. Wiggins, J. Bonse, J. Solis, C. N. Afonso, K. Sokolowski-Tinten, V. V. Temnov, P. Zhou, and D. von der Linde, J. Appl. Phys. **98**, 113518 (2005).
[9] H. Huang, F. Zuo, F. Zhai, Y. Wang, T. Lai, Y. Wu, and F. Gan, J. Appl. Phys. **106**, 063501 (2009).
[10] J. K. Olson, H. Li, T. Ju, J. M. Viner, and P. C. Taylor, J. Appl. Phys. **99**, 103508 (2006).
[11] M. Wuttig, D. Luesebrink, D. Wamwangi, W. Welnic, M. Gillessen, and R. Dronskowski, Nature Mater. **6**, 122 (2007).
[12] A. V. Kolobov, P. Fons, A. I. Frenkel, A. L. Ankudinov, J. Tominaga, and T. Uruga, Nature Mater. **3**, 703 (2004).

Downloaded 29 Oct 2012 to 161.111.22.141. Redistribution subject to AIP license or copyright; see http://jap.aip.org/about/rights_and_permissions

[13]J. Siegel, W. Gawelda, D. Puerto, C. Dorronsoro, J. Solis, C. N. Afonso, J. C. G. De Sande, R. Bez, A. Pirovano, and C. Wiemer, J. Appl. Phys. **103**, 023516 (2008).
[14]J. Siegel, C. N. Afonso, and J. Solis, Appl. Phys. Lett. **75**, 3102 (1999).
[15]J. Siegel, A. Schropp, J. Solis, C. N. Afonso, and M. Wuttig, Appl. Phys. Lett. **84**, 2250 (2004).
[16]N. Yamada, E. Ohno, K. Nishiuchi, N. Akahira, and M. Takao, J. Appl. Phys. **69**, 2849 (1991).
[17]E. Huber and E. E. Marinero, Phys. Rev. B **36**, 1595 (1987).
[18]Y. Nakayoshi, Y. Kanemitsu, Y. Masumoto, and Y. Maeda, Jpn. J. Appl. Phys. **31**, 471 (1992).
[19]A. L. Lacaita, D. Ielmini, and D. Mantegaza, Solid-State Electron. **52**, 1443 (2008).
[20]S. Raoux, H.-Y. Cheng, M. A. Caldwell, and H.-S. P. Wong, Appl. Phys. Lett. **95**, 071910 (2009).
[21]A. Abrutis, V. Plausinaitiene, M. Skapas, C. Wiemer, W. Gawelda, J. Siegel, and S. Rushworth, J. Cryst. Growth **311**, 362 (2009).
[22]J. Solis, J. Siegel, and C. N. Afonso, Rev. Sci. Instrum. **71**, 1595 (2000).
[23]A. Abrutis, V. Plausinaitiene, M. Skapas, C. Wiemer, O. Salicio, A. Pirovano, E. Varesi, S. Rushworth, W. Gawelda, and J. Siegel, Chem. Mater. **20**, 3557 (2008).
[24]O. Salicio, C. Wiemer, M. Fanciulli, W. Gawelda, J. Siegel, C. N. Afonso, V. Plausinatiene, and A. Abrutis, J. Appl. Phys. **105**, 033520 (2009).
[25]P. L. Liu, R. Yen, N. Bloembergen, and R. T. Hodgson, Appl. Phys. Lett. **34**, 864 (1979).
[26]T. C. Chong, L. P. Shi, X. S. Miao, P. K. Tan, R. Zhao, and Z. P. Cai, Jpn. J. Appl. Phys. **39**, 737 (2000).
[27]M. Wuttig and C. Steimer, Appl. Phys. A **87**, 411 (2007).

Downloaded 29 Oct 2012 to 161.111.22.141. Redistribution subject to AIP license or copyright; see http://jap.aip.org/about/rights_and_permissions